SPANDIDOS PUBLICATIONS

ONCOLOGY LETTERS 25: 207, 2023

Increased soluble E-cadherin of spheroid formation supplemented with fetal bovine serum in colorectal cancer cells

IN-YOUB CHANG[1] and SANG-PIL YOON[2]

[1]Department of Anatomy, College of Medicine, Chosun University, Gwangju 61452; [2]Department of Anatomy, College of Medicine, Jeju National University, Jeju 63243, Republic of Korea

Received December 7, 2022; Accepted March 23, 2023

DOI: 10.3892/ol.2023.13793

Abstract. Cancer stem cells (CSCs) are known to be a major cause of metastasis, resistance and recurrence. Spheroid formation is one of the methods used to recruit CSCs utilizing an anchorage-independent environment *in vitro*. It was aimed to investigate the availability of spheroid formation culture methods in the research field of CSCs and resistance using 5-fluorouracil (5-FU)-resistant colorectal cancer cells. The wild type SNU-C5 and 5-FU-resistant SNU-C5 (SNU-C5/5-FUR) cells were cultured as usual (monolayer), and in 3-dimensional non-adhesive environments supplemented with fetal bovine serum (FBS) or growth factors, respectively. The characteristics of the spheroids were evaluated by morphometry, cell viability assay, western blotting, immunocytochemistry and enzyme-linked immunosorbent assay. Spheroid formation was induced in an environment supplemented with FBS, while SNU-C5/5-FUR cells only formed spheres in media supplemented with GFs. Sphere-formed cells showed slower cell proliferation than cells from monolayer, which coincided with an increased level of p21 and a decreased level of β-catenin. Markers for CSCs and drug resistance were not significantly changed after spheroid formation. Sphere-formed cells showed significantly increased levels of soluble E-cadherin, particularly in the environment supplemented with FBS. These results suggested that spheroid formation may be related to soluble E-cadherin, but is not related to CSCs or resistance markers.

Introduction

Colorectal cancer (CRC) is the third-most common cancer, accounting for 10.2% of new diagnoses as well as the second-leading cause of cancer-related mortality, accounting for 9.2% worldwide (1,2). Although adjuvant and neo-adjuvant chemotherapy are standard front-line approaches in support of surgery, 5-fluorouracil (5-FU), one of the original fluoropyrimidines, has been considered a mainstay of chemotherapy for CRC (3,4). A recent review (5) summarized the various mechanisms against 5-FU including the alterations in drug transport, changes in the cell cycle, epithelial-to-mesenchymal transition (EMT), and cancer stem cell (CSC) involvement. Certain resistance mechanisms that are 5-FU-specific have also been ascertained in 5-FU-resistant SNU-C5 (SNU-C5/5-FUR) CRC cells as compared with wild type SNU-C5 cells to include the upregulation of cyclooxygenase-2 derived prostaglandin E2 (6) and over-activation of protein kinase B (Akt) (7,8). The differential activation of extracellular signal-regulated protein kinase (ERK) between wild type and 5-FU-resistant CRC cells after yeast extract treatment has been previously suggested by the authors (8). It has also been reported that SNU-C5/5-FUR cells are more susceptible to an aqueous extract of *Orostachys japonica* A. Berger than wild type SNU-C5 cells via the activation of mitogen-activated protein kinase signaling pathways including ERK and p38 (9).

Although the CSC markers between cancers are not identical (10), CSCs exhibit common characteristics regarding the maintenance of CSC pool, tumorigenesis, metastasis, and treatment resistance and recurrence (11-13). As p21 attenuates Ras- and c-Myc-dependent EMT and CSC-like gene expression *in vivo* (14), it suppresses the cell cycle and is also used as a biomarker for CSCs (15). Similarly, the Wnt/β-catenin signaling pathway is critical for the regulation of cell proliferation, differentiation and apoptosis during regeneration (16). CSCs are typically determined by the cell surface proteins [cluster of differentiation (CD) 44, and nuclear transcription factors, octamer binding transcription factor-4 (Oct-4), and sex determining region Y-box-2 (Sox-2)] (13,17) as well as ATP-binding cassette super-family G member 2 (ABCG2) transporter (18). Moreover, non-CSCs can acquire a CSC-like phenotype during EMT (19), and EMT-induced cells can form spheres in an anchorage-independent growth environment (20).

The three-dimensional (3D) tumor spheroid formation model has been suggested to be an essential tool for confirming CSC-like features *in vitro* (21), because it resembles *in vivo* solid tumors rather than the conventional, two-dimensional (2D) monolayer culture (22). Although various methods and conditions have been proposed, spheroids consist of an external proliferating zone, an internal quiescent zone, and a

Correspondence to: Dr Sang-Pil Yoon, Department of Anatomy, College of Medicine, Jeju National University, 102 Jejudaehak-ro, Jeju-Si, Jeju-Do 63243, Republic of Korea
E-mail: spyoon@jejunu.ac.kr

Key words: colon cancer, cancer stem cell, drug resistance, E-cadherin, spheroid formation

necrotic core (22). During the spheroid formation process in any environment, it is known that cells initially aggregate and then form compact spheroids via E-cadherin (22). E-cadherin, an epithelial cell to cell adhesion molecule, is inversely correlated with EMT (23). Although E-cadherin is also known to be frequently downregulated with tumorigenesis, cell adherence between cancer cells are disturbed by addition of the soluble fragment (80 kDa) of E-cadherin, leading to malignancy in cancers (24,25).

Growth factors (GFs) have been used in spheroid formation culture methods to maintain the integrity of CSCs (17,22), which is also applied to CRC cells in order to effectively obtain CSCs to date (26,27). Although fetal bovine serum (FBS) supplementation has recently been suggested as an adaptable, efficient, and cost-effective tool to maintain pluripotency in a hepatocellular carcinoma cell (28), it has not been investigated in acquired drug-resistant CRC cells. Therefore, it was aimed to investigate whether spheroid formation culture depend on supplementations is appropriate on acquired 5-FU-resistant SNU-C5/5-FUR CRC cells as compared with wild type SNU-C5 cells. Spheroid formation culture methods with different culture environments supplemented with FBS and GFs, respectively, were used. Accordingly, the feasibility of appropriate spheroid formation culture methods was examined in each of different CRC cell, and the differences between wild type and acquired 5-FU-resistance were revealed.

Materials and methods

Antibodies. The antibodies specific for β-catenin (1:1,000; cat. no. sc-7199), c-Myc (9E10; 1:1,000; cat. no. sc-40), E-cadherin (H-108; 1:1,000; cat. no. sc-7870), epithelial cell adhesion molecule (EpCAM) (c-10; 1:1,000; cat. no. sc-25308), glyceraldehyde 3-phophage dehydrogenase (GAPDH; 1:2,000; cat. no. sc-47724), glycogen synthase kinase-3 beta (GSK-3β; 1:1,000; cat. no. sc-9166), Oct3/4 (C-10; 1:1,000; cat. no. sc-5279), Pan-Ras (C-4; 1:1,000; cat. no. sc-166691), Sox2 (E-4; 1:1,000; cat. no. sc-365823) and Wilms tumor protein [WT1 (6F-H17); 1:1,000; cat. no. sc-81619] were obtained from Santa Cruz Biotechnology, Inc. cAMP response element-binding protein (CREB) [phosphor S133 (E113); 1:1,000; cat. no. ab32096], CD24 [M1/69] (1:1,000; cat. no. ab64064), and CD44 (1:1,000; cat. no. ab157107) were obtained from Abcam. ABCG2 (BCRP1, clone 5D3; cat. no. MAB4155; 1:500) and α-smooth muscle actin (αSMA; 1:2,000; cat. no. A2547) from were obtained MilliporeSigma. CREB (1:1,000; cat. no. CSB-PA005947HA01HU; Cusabio Technology, LLC), fibronectin (1:2,000; cat. no. CL54951AP; Cedarlane Laboratories), p21 (1:1,000; cat. no. 60214-1; Proteintech Group, Inc.) and p90RSK (Ab348; 1:1,000; cat. no. 79-554; Prosci, Inc.) were obtained from the corresponding listed company.

Cell culture. SNU-C5 (Korean Cell Line Bank; Seoul, South Korea) and SNU-C5/5-FUR (Research Center for Resistant Cells; Chosun University, Gwangju, South Korea) cells were cultured in RPMI-1640 medium supplemented with 10% heat-inactivated FBS, 100 U/ml penicillin and 100 mg/ml streptomycin at 37°C (Welgene, Inc.) in a humidified atmosphere with 5% CO_2 as previously described (8).

Spheroid formation. 96-well plates were covered with poly-2-hydroxyethylmethacylate (cat. no. P3932; Sigma-Aldrich; Merck KGaA) to create an anchorage-independent environment. Cells were cultured with 1% B27 supplement (cat. no. 17504-044), 20 ng/ml epidermal GF (cat. no. PHG0311) and 20 ng/ml basic fibroblast GF (cat. no. 13256029; all from Thermo Fisher Scientific, Inc.) in DMEM/F12 medium (sphere/GF group) (17,21), or in same culture media with FBS (sphere/FBS group) as previously reported (28). Spheroid formation was checked for morphometry on days 7, 14 and 28.

Cell viability assay. The effect of 5-FU on cell viability was evaluated in terms of the reduction of MTT (Amresco, LLC) using a VERSAmax microplate reader (Molecular Devices, LLC) as previously described (10,19). Dissociated cells from 2D monolayer and spheroid-formation cultures with trypsin-EDTA (Welgene, Inc.) were seeded in triplicate wells in 96-well plates ($2x10^3$ cells/well), and treated with 5-FU at various concentrations as previously described (22). The number of viable cells was estimated for 3 days after incubation in 2D culture, and for 4 days after incubation in spheroid formation culture methods. The effect of the drug was calculated and compared with untreated (DMSO-treated only) cells using Microsoft Excel (MS Office 2016).

Western blotting. Cells were incubated for 3 days in monolayer culture, and incubated in spheroid formation culture for 4 weeks. Cells were harvested in M-PER mammalian protein extraction reagent (Thermo Fisher Scientific, Inc.) including 1% protease inhibitor cocktail set III (EMD Millipore), 0.5% phosphatase inhibitor cocktail 2 and 0.5% phosphatase inhibitor cocktail 3 (both from Sigma-Aldrich; Merck KGaA). Protein concentration was assessed using BCA protein assay (Thermo Fisher Scientific, Inc.) according to the manufacturer's instructions.

The electrophoresis of protein in cell lysates on an TGX Stain-Free FastCast™ Acrylamide Starter kit (Bio-Rad Laboratories, Inc.) using tris/glycine buffer systems (Bio-Rad Laboratories, Inc.) onto PVDF membranes was performed as previously described (8,17). The membranes were first blocked at room temperature with 5% skim milk for 1 h and then incubated with primary antibodies overnight at 4°C. After washing, peroxidase anti-mouse or anti-rabbit IgG antibodies (1:3,000; cat. no. PI-2,000 and PI-1,000, Vector Laboratories, Inc.) were applied for 1 h at room temperature. Next, western lighting chemiluminescence reagent (PerkinElmer, Inc.) was used to detect proteins. The anti-GAPDH antibody was used as a loading control on the stripped membranes. The bands were captured using Azure™ c300 (Azure Biosystems, Inc.) and quantified using the AzureSpot analysis software (version 14.2; Azure Biosystems, Inc.).

Enzyme-linked immunosorbent assay (ELISA). ELISA was performed according to the manufacturer's instruction (Human E-cadherin SimpleStep ELISA Kit, cat. no. ab233611; Abcam). Briefly, standard and spheroid formation culture media samples were added into each well to bind E-cadherin antibody cocktail followed by incubation of 1 h at room temperature. After being washed with washing

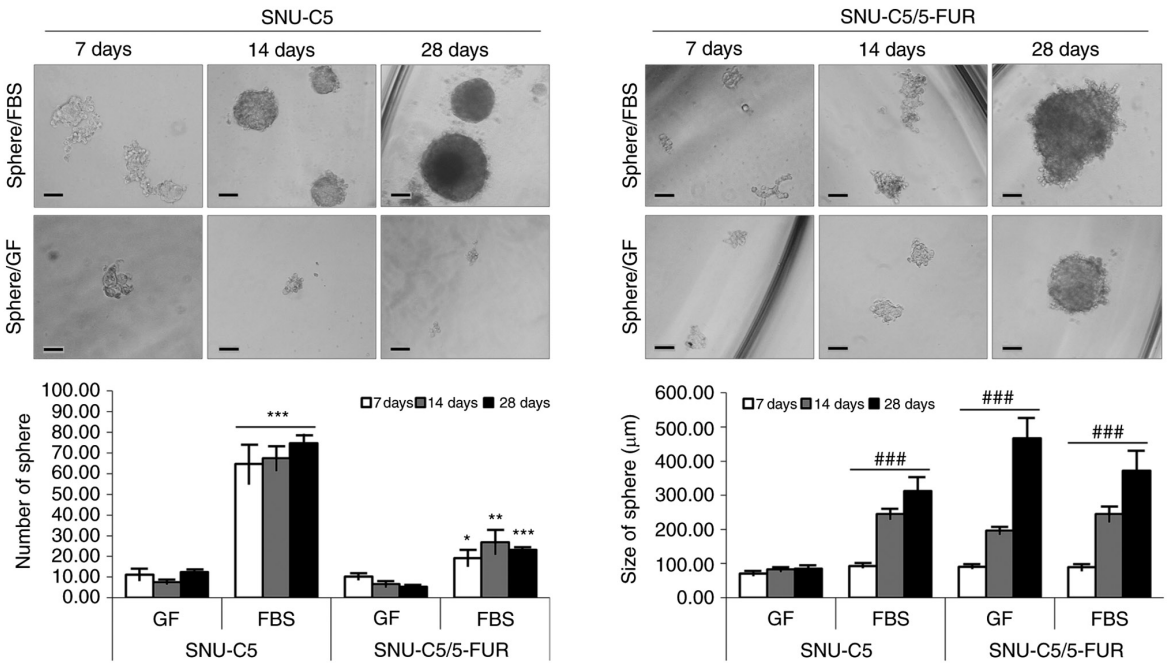

Figure 1. Spheroid formation of CRC cells in different environments. The wild type SNU-C5 and 5-FU-resistant SNU-C5 (SNU-C5/5-FUR) CRC cells were cultured in an anchorage-independent condition supplemented with FBS or GF. The number and size (diameter) of spheres were estimated at 7, 14 and 28 days after seeding. Data are presented as the mean ± SD (n=3). Scale bar, 100 μm. *P<0.05, **P<0.01 and ***P<0.001 vs. GF; $^{###}$P<0.001 vs. p7. CRC, colorectal cancer; FBS, fetal bovine serum; GF, growth factor.

buffer, TMB1 substrate reagent was added into each well and incubated for 10 min. At this point, the stop solution was added and optical density was measured at 450 nm using a VERSAmax microplate reader.

Immunocytochemistry. Four weeks after spheroid formation e culture, the formed spheres were fixed for 24 h at 4˚C in 4% paraformaldehyde, and 4 μm-thick-sections were prepared for immunocytochemistry. The sections were blocked with 10% normal horse serum (cat. no. MP-7401; Vector) for 1 h at room temperature. Incubation with the anti-E-cadherin antibody (1:100) was performed for overnight at 4˚C. The binding was visualized using an anti-rabbit secondary antibody (1:200; cat. no. MP-7401; Vector), and the nuclei were counterstained with hematoxylin (cat. no. H-3404, Vector) for 1 min at room temperature.

Statistical analysis. All data were compiled from a minimum of three replicate experiments. Data are expressed as the mean values ± SD. P<0.05 was considered to indicate a statistically significant difference as determined using the Student's paired t-test or one-way ANOVA followed by a Bonferroni post-hoc test. MS Excel 2016 was used for statistical analysis.

Results

Spheroid formation in different environments supplemented with FBS or GF. To evaluate the tumorigenic capacities of SNU-C5 and SNU-C5/5-FUR CRC cells, the cells were cultured in an anchorage-independent condition for 4 weeks. Both cell lines successfully formed spheres in the FBS-supplemented environment. SNU-C5/5-FUR cells only formed spheres in the GF-supplemented environment. The mean size of each cell was significantly increased with the passage of time (P<0.001) (Fig. 1 and Table I).

Cell viability and proliferation of spheroid formation in different environments supplemented with FBS or GF. To investigate the proliferation and acquisition of drug resistance in spheroid formation, the effect of an anticancer drug (5-FU) on cell viability was assessed using the MTT assay. Spheroid-formed cells from SNU-C5 cells revealed higher cell viability to 5-FU at 10 (P=0.0174 in sphere/GF; P=0.0421 in sphere/FBS) and 100 μM (P=0.0030 in sphere/GF; P=0.0162 in sphere/FBS) compared with the cells from monolayer culture. The difference in cell viability between environments (sphere/GF vs. sphere/FBS) was statistically significant (P=0.0421/10 μM; P=0.0455/100 μM). Resistance-acquired SNU-C5/5-FUR cells did not show any change to 5-FU with spheroid formation (Fig. 2A). Sphere-formed cells demonstrated significantly slower proliferation than those in monolayer, wherein sphere-formed cells reached the same level at 4 days of incubation when original cells reached proliferation level at 3 days of incubation (8). In addition, sphere-formed cells in GF-supplemented environment showed relatively slower proliferation than those in FBS-supplemented environment (Fig. 2B).

To delineate the characteristics of spheroid-formed cells, the levels of p21, β-catenin and GSK3β were first measured to confirm the feasible mechanisms of slower proliferation (Fig. 2C and Table II). Compared with monolayer culture, p21 was increased in both CRC cells. Whereas β-catenin was found to be decreased in both CRC cells, GSK3β was decreased in FBS-supplemented environments and sustained in GF-supplemented environment (P=0.0046 between environments).

Table I. Number and size (μm) of spheres in GF- and FBS-supplemented environments of SNU-C5 and SNU-C5/5-FUR cells.

	SNU-C5			SNU-C5/5-FUR		
Variables	Sphere/GF	Sphere/FBS	P-value	Sphere/GF	Sphere/FBS	P-value
No.						
D7	11.08±2.57	64.67±9.35	<0.001	10.25±1.27	19.25±3.72	<0.0309
D14	7.46±0.77	67.46±5.77	<0.001	6.58±1.36	26.88±5.74	<0.0069
D28	12.39±1.21	74.78±4.00	<0.001	5.28±0.35	23.17±0.52	<0.001
Size (μm)						
D7	71.25±5.12	93.09±3.16	-	90.30±3.13	89.00±8.33	-
D14	82.59±4.72	245.36±15.08[a]	<0.001	197.04±10.24[a]	245.06±22.03[a]	<0.001
D28	85.50±5.04	312.34±41.14[a]	<0.001	467.19±59.78[a]	371.57±55.88[a]	<0.001

The numbers of spheres were compared between environments. [a]The sizes of the spheres were compared with the previous time point (P<0.05). D, days of incubation; FBS, fetal bovine serum; GF, growth factor.

Cellular and molecular markers of spheroid formation in different environment supplemented with FBS or GF. CSC markers were assessed in the spheroid-formed cells to reveal the stemness (Fig. 3A and Table II). Compared with monolayer culture, pan-Ras was significantly increased while other markers were decreased in SNU-C5 cells. In the case of SNU-C5/5-FUR cells, pan-Ras and WT1 were increased in sphere/GF environment but decreased in sphere/FBS environment, and considerable differences were observed between supplementations (P<0.001/each). Oct3/4 and Sox2 were decreased or sustained.

Next, drug resistance-related markers were assessed in the spheroid-formed cells (Fig. 3B and Table II). Compared with monolayer culture, ABCG2, p90RSK, phosphorylated (p)-CREB and CREB were all decreased or unchanged in SNU-C5 cells. Regarding SNU-C5/5-FUR cells, p90RSK was increased in GF-supplemented environment and pCREB was increased in FBS-supplemented environment. The other markers were decreased or unchanged in sphere-forming cells.

Surface markers related to stemness and/or EMT were also assessed in the spheroid-formed cells (Fig. 3C and Table II). Compared with monolayer culture, epithelial CD24 and mesenchymal CD44 were decreased in spheres in both CRC cells. The ratio between CD44/CD24, which is useful data for searching CSCs, was significantly decreased in sphere/FBS (0.30±0.02-fold in SNU-C5 cells, 0.24±0.06-fold in SNU-C5/5-FUR cells; P<0.001/each) and in sphere/GF (0.65±0.08 fold; P=0.0048). There was a significant difference between supplementations (P=0.0013) in SNU-C5/5-FUR cells.

Differential expression of EMT markers of spheroid formation in different environment supplemented with FBS or GF. As the spheroid formation culture method inhibits the adhesion of cells to the base of culture dish, the EMT markers were assessed (Fig. 4A and Table II). Compared with the monolayer culture, fibronectin was significantly increased in FBS-supplemented environment in both CRC cells but decreased in GF-supplemented environment in SNU-C5/5-FUR cells (P<0.001 between environments). EpCAM and αSMA were not changed in the spheroid formation culture. Compared with monolayer culture, 135-120 kDa E-cadherin was decreased in all spheroid formation conditions that were examined in this experiment. Soluble E-cadherin (80 kDa) was significantly increased in the FBS-supplemented environment in both CRC cells, but sustained in the GF-supplemented environment of SNU-C5/5-FUR cells (Fig. 4B and Table II). The ratio of soluble to 135-120 kDa E-cadherin was significantly increased in FBS-supplemented environment in SNU-C5 (2.50±0.49-fold; P=0.0062) and in SNU-C5/5-FUR (4.64±0.42-fold; P<0.001) cells. The ratio was sustained in sphere/GF (1.06±0.08-fold), while there was a significant difference between supplementations (P<0.001) in SNU-C5/5-FUR cells.

The concentration of E-cadherin in cultured media of SNU-C5 and SNU-C5/5-FUR cells in 2D monolayer, sphere/FBS, and sphere/GF group were estimated by ELISA (Fig. 4C). The ratio of soluble E-cadherin was found to be significantly increased in 28 days of incubation in sphere/FBS compared with 2D monolayer (3 days of incubation) and with 7 days of incubation in sphere/FBS environment in SNU-C5 cells (25.47±1.98-fold vs. monolayer, P<0.001), and in SNU-C5/5-FUR cells (4.48±0.50-fold vs monolayer, P<0.001), respectively. However, the ratio of E-cadherin was not changed until 28 days after incubation in GF-supplemented environments in both CRC cells.

The morphological features were evaluated by the expression of E-cadherin (Fig. 4D). E-cadherin was immunostained on the cell membrane of spheroid-formed cells in both CRC cells with GF and FBS supplementations. Some central area was neither immunostained with E-cadherin, nor stained with hematoxylin for nuclei.

Discussion

The efficiency of spheroid formation is known to differ between cell lines, even within the same tumor type (22), which was also observed in a recent study by the authors (17). It was found that the spheroid formations of both CRC cell lines were induced in an improved manner when supplemented with

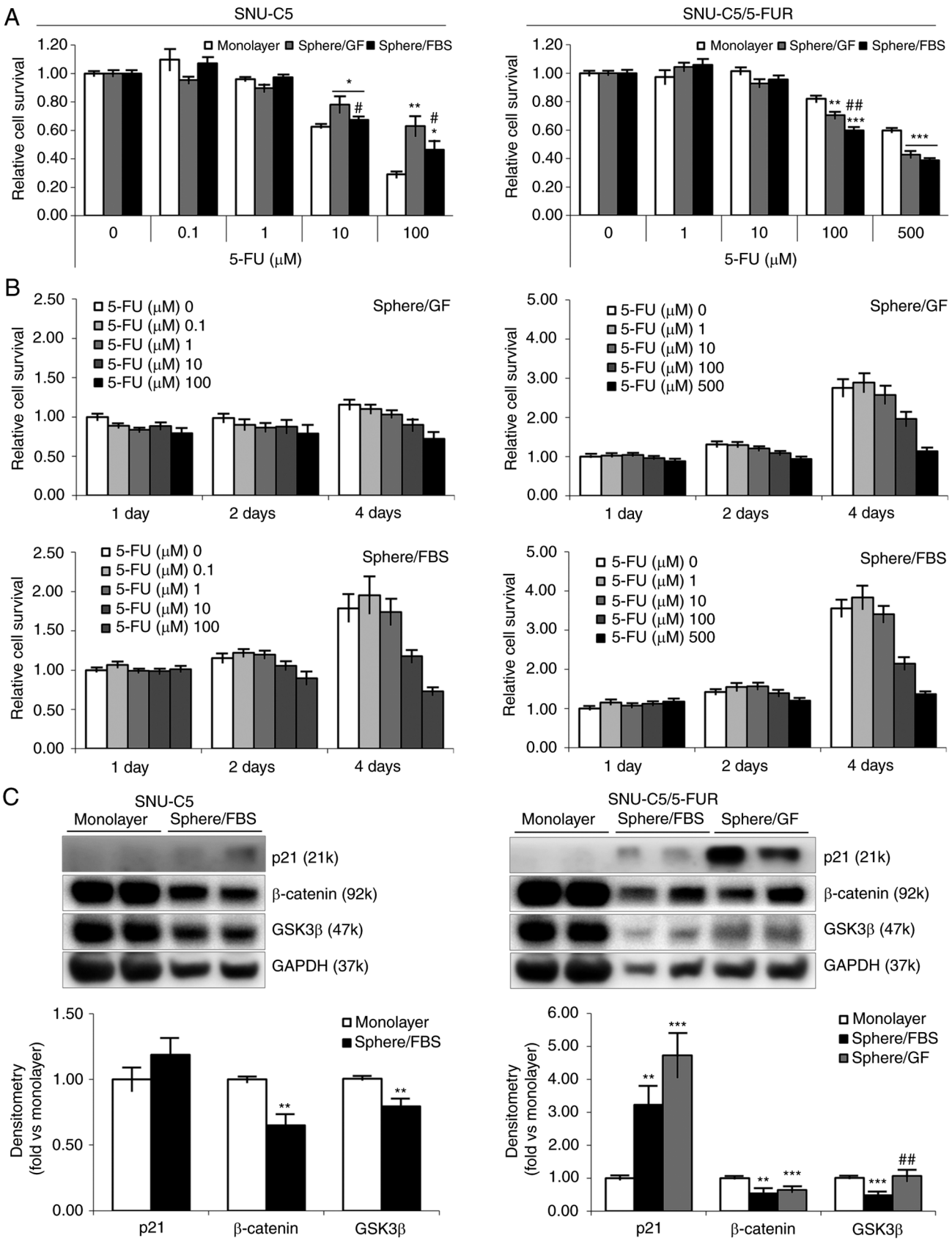

Figure 2. Cell viability changes after spheroid formation of colorectal cancer cells in different environments. (A) The SNU-C5 and SNU-C5/5-FUR cells were mock-treated with DMSO or treated with indicated doses of 5-FU for 3 days. The extent of cell viability was determined by MTT assay. Data are presented as the mean ± SD (n=3). *P<0.05, **P<0.01 and ***P<0.001 vs. DMSO; $^{\#}$P<0.05 and $^{\#\#}$P<0.01 vs. sphere/GF. (B) The SNU-C5 and SNU-C5/5-FUR cells were mock-treated with DMSO or treated with indicated doses of 5-FU for indicated days. The extent of cell viability was determined by MTT assay using the aforementioned procedures. Data are presented as the mean ± SD (n=3). (C) Expression levels of cell cycle-related proteins in monolayer and spheroid formation cultures in SNU-C5 and SNU-C5/5-FUR cells were detected by immunoblotting. Immunoblotting analysis was performed for p21, β-catenin and GSK3β, while GAPDH was used for a loading control. Band density was analyzed by AzureSpot analysis software, and results are expressed as the mean ± SD (n=3). **P<0.01 and ***P<0.001 vs. monolayer; $^{\#\#}$P<0.01 vs. sphere/FBS. 5-FU, 5-fluorouracil; FBS, fetal bovine serum; GF, growth factor.

Table II. Densitometric results of western blotting on SNU-C5 and SNU-C5/5-FUR cells.

	SNU-C5			SNU-C5/5-FUR		
Variables	Sphere/FBS	P-value	Sphere/FBS	P-value	Sphere/GF	P-value
Proliferation						
p21	1.19±0.13	0.1248	3.22±0.57	0.0015	4.73±0.67	<0.001
β-catenin	0.65±0.09	0.0013	0.54±0.14	0.0043	0.64±0.07	0.0014
GSK3β	0.80±0.06	0.0032	0.48±0.06	<0.001	1.06±0.16	0.3696
Stemness						
pan-Ras	1.38±0.04	0.0065	0.71±0.07	0.0011	1.24±0.06	0.0013
Oct3/4	0.90±0.04	0.0948	0.61±0.07	<0.001	1.09±0.08	0.1597
Sox2	0.64±0.08	0.0019	0.49±0.03	<0.001	0.61±0.05	<0.001
WT1	0.88±0.05	0.0158	0.50±0.05	<0.001	1.35±0.08	0.0005
Drug resistance						
ABCG2	0.64±0.05	<0.001	0.85±0.10	0.0982	0.72±0.12	0.0284
P90RSK	0.80±0.08	0.0370	0.97±0.21	0.4514	1.39±0.05	<0.001
pCREB	0.96±0.17	0.4190	1.33±0.16	0.0473	0.92±0.10	0.2358
CREB	0.82±0.05	0.0073	0.67±0.08	<0.001	0.81±0.14	0.0800
Surface marker						
CD44	0.21±0.01	<0.001	0.16±0.03	<0.001	0.60±0.07	<0.001
CD24	0.69±0.03	<0.001	0.73±0.07	0.0075	0.94±0.08	0.2360
EMT						
Fibronectin	4.90±0.73	<0.001	11.57±2.15	<0.001	0.67±0.10	0.0094
EpCAM	0.33±0.08	<0.001	0.11±0.03	<0.001	0.20±0.08	<0.001
αSMA	0.71±0.03	0.0095	0.51±0.06	<0.001	1.01±0.15	0.4869
E-cadherin						
135-120 kDa	0.88±0.12	0.1727	0.55±0.13	0.0073	0.83±0.10	0.0873
80 kDa	3.80±0.70	0.0013	4.52±0.96	0.0054	0.70±0.10	0.0550

Each result was first normalized by GAPDH and then compared with the results obtained from 2D monolayer culture as a standard. Results are shown in terms of the relative fold with p value, and GF- and FBS-supplemented environments were also compared in SNU-C5/5-FUR cells. EMT, epithelial-to-mesenchymal transition; FBS, fetal bovine serum; GF, growth factor; EpCAM, epithelial cell adhesion molecule.

FBS compared with GFs, while SNU-C5/5-FUR cells only formed spheres supplemented with GFs. Sphere-formed cells showed 5-FU resistance in SNU-C5 cells irrespective of the supplementations used as previously suggested (22). However, SNU-C5/5-FUR cells did not show any further changes against 5-FU in spheroid formation culture. Sphere-formed cells showed slower cell proliferation than cells from monolayer culture, which coincided with an increased level of p21 and a decreased level of β-catenin as previously reported (19,21,22). However, cellular and molecular markers for CSCs, drug resistance, and EMT were not significantly changed between 2D and 3D culture conditions although the cells could acquire CSC-like phenotype via EMT to form spheres (19,20). As a result, spheroid formation culture methods are not appropriate to study CSCs or drug resistance in acquired 5-FU-resistant CRC cells, at least in long-term maintenance condition. Notably, spheroid formation supplemented with FBS environment showed significantly increased level of soluble E-cadherin.

GFs were used in spheroid formation culture methods (17,22,26,27). The suitability of spheroid formation culture methods has been investigated, and the results of such studies have revealed that cancer cells showed differential efficiency of spheroid formation, where the efficiency differed depending on cell lines even for the same tumor type (22). SNU-C5/5-FUR cells showed variable morphology of spheroids in different environments, wherein complete spheroids were formed in GF-supplemented environment with smaller numbers than those formed in FBS-supplemented environment. Although the spheroids in GF-supplemented environment did not acquire further drug resistance, they exhibited increased CSC markers compared with monolayer or FBS-supplemented spheroids. Accordingly, drug-resistance-acquired cells were not suitable for spheroid formation culture methods to investigate CSCs depending on drug resistance, at least in SNU-C5/5-FUR cells. As FBS supplementation was suggested for the *in vitro* cultivation of CSCs (28), spheroid formation was easily induced and maintained for up to 4 weeks in FBS-supplemented environment in both CRC cells. The spheres showed acquired drug resistance, slow proliferation, and increased level of pan-Ras. However, further changes on cellular and molecular markers of CSCs,

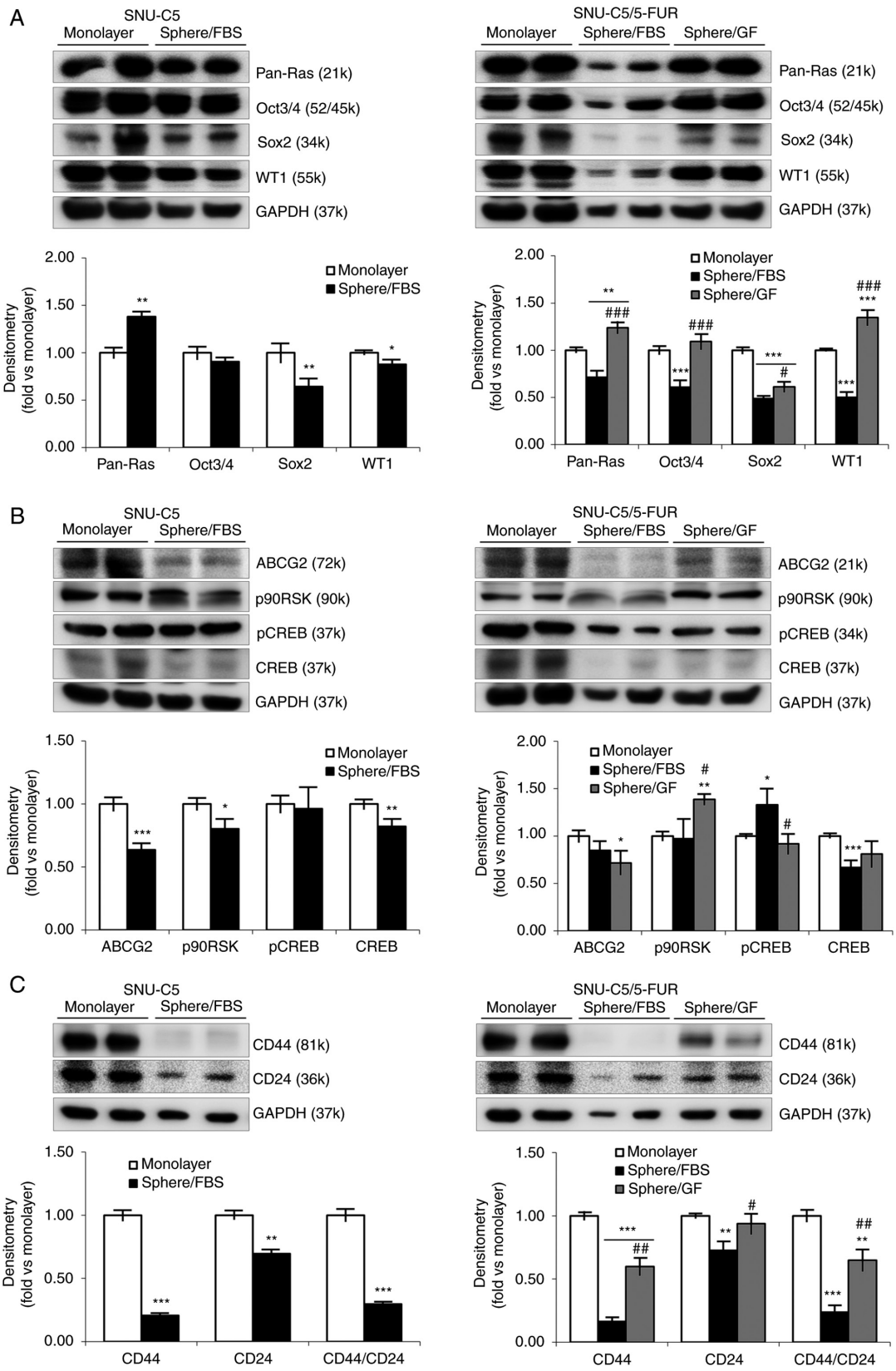

Figure 3. Cellular and molecular markers for CSCs and drug resistance on spheroid formation of colorectal cancer cells in different environments. (A) Expression levels of CSC markers in monolayer and spheroid formation cultures in SNU-C5 and SNU-C5/5-FUR cells were detected by immunoblotting. Immunoblotting analysis was performed for pan-Ras, Oct3/4, Sox2 and WT1, while GAPDH was used for a loading control. Band density was analyzed by AzureSpot analysis software, and results are expressed as the mean ± SD (n=3). (B) Expression levels of drug efflux markers in monolayer and spheroid formation cultures in SNU-C5 and SNU-C5/5-FUR cells were detected by immunoblotting. Immunoblotting analysis was performed for ABCG2, p90RSK, pCREB, and CREB, while GAPDH was used for a loading control. Band density was analyzed by AzureSpot analysis software, and results are expressed as the mean ± SD (n=3). (C) Expression levels of cell surface markers in monolayer and spheroid formation cultures in SNU-C5 and SNU-C5/5-FUR cells were detected by immunoblotting. Immunoblotting analysis was performed for CD44 and CD24, while GAPDH was used for a loading control. Band density was analyzed by AzureSpot analysis software, and results are expressed as the mean ± SD (n=3). *P<0.05, **P<0.01 and ***P<0.001 vs. monolayer; $^{\#}$P<0.05, $^{\#\#}$P<0.01 and $^{\#\#\#}$P<0.001 vs. sphere/FBS. CSCs, cancer stem cells; FBS, fetal bovine serum; GF, growth factor; p-, phosphorylated.

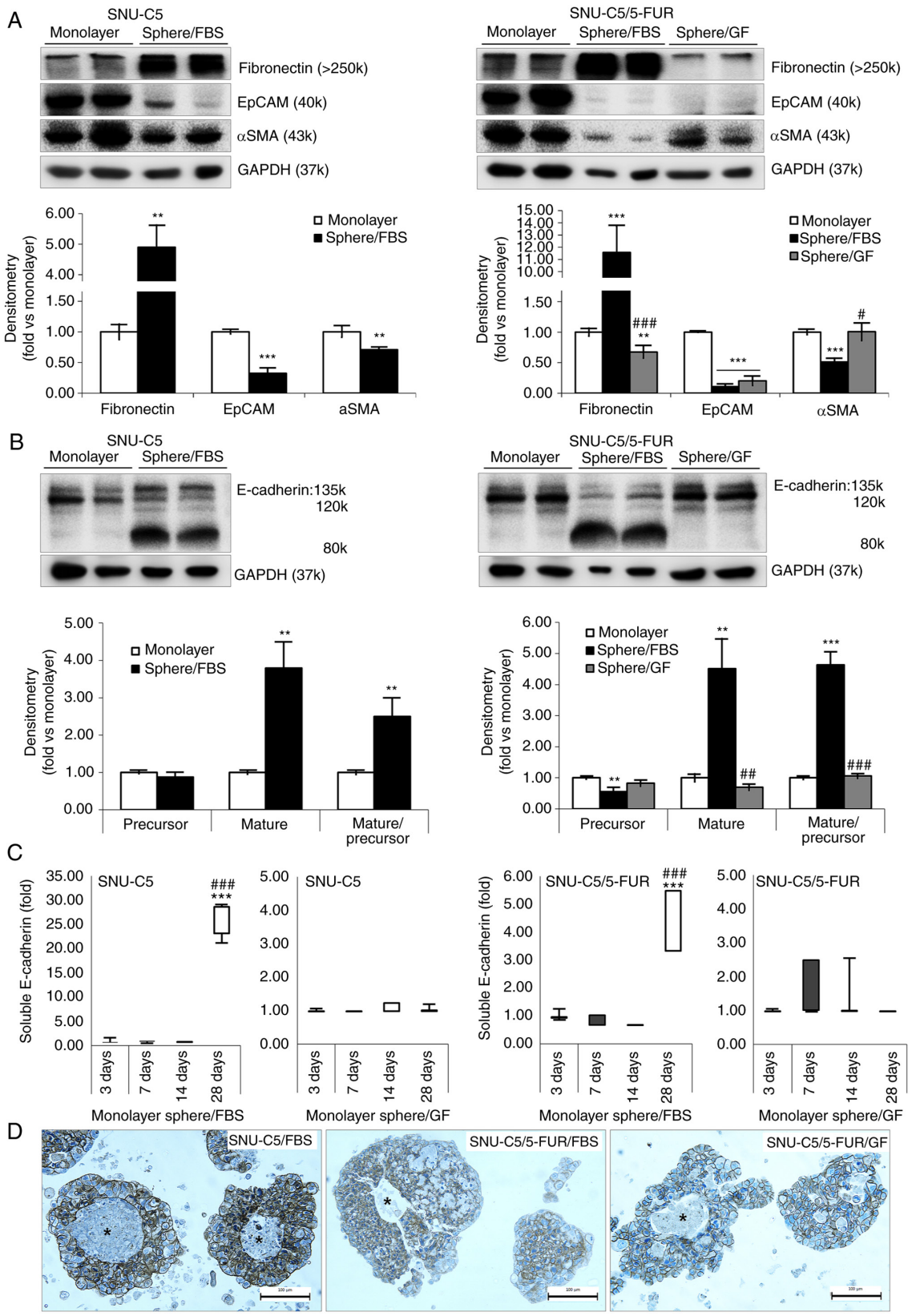

Figure 4. Markers for EMT on spheroid formation of colorectal cancer cells in different environments. (A) Expression levels of EMT markers in monolayer and spheroid formation cultures in SNU-C5 and SNU-C5/5-FUR cells were detected by immunoblotting. Immunoblotting analysis was performed for fibronectin, EpCAM and αSMA, while GAPDH was used as a loading control. Band density was analyzed by AzureSpot analysis software, and results are expressed as the mean ± SD (n=3). (B) Expression of E-cadherin in monolayer and spheroid formation cultures in SNU-C5 and SNU-C5/5-FUR cells was detected by immunoblotting. Immunoblotting analysis was performed for E-cadherin, which was subdivided into 135 -120 kDa and soluble 80 kDa fractions, while GAPDH was used as a loading control. Band density was analyzed by AzureSpot analysis software, and results are expressed as the mean ± SD (n=3). (C) Enzyme-linked immunosorbent assay of E-cadherin on culture media in SNU-C5 and SNU-C5/5-FUR cells. Data are presented as the mean ± SD (n=3). (D) Immunocytochemical staining of E-cadherin on spheroid formation in SNU-C5 and SNU-C5/5-FUR cells. Asterisks indicate areas that were neither immunostained with E-cadherin, nor stained with hematoxylin (Scale bar, 100 μm). **P<0.01 and ***P<0.001 vs. monolayer; $^{\#}$P<0.05, $^{\#\#}$P<0.01 and $^{\#\#\#}$P<0.001 vs. sphere/FBS. EMT, epithelial-to-mesenchymal transition; FBS, fetal bovine serum; GF, growth factor; EpCAM, epithelial cell adhesion molecule.

drug resistance, surface protein, and EMT were not observed. Therefore, FBS-supplemented environment was not considered to be such an effective tool for CSCs in CRC cells, at least in SNU-C5/5-FUR cells and in long-term maintenance.

During the spheroid formation process in any environment, it is known that cells initially aggregate and then form compact spheroids via a high level of E-cadherin (22). However, expression of E-cadherin was reported as 'decrease' in CSC, as induced by spheroid formation culture methods, of the colon (29,30), breast (31,32), liver (33), pancreas (34), and oral and prostate (35) cancers with variable vendors in short-term maintenance. Previous studies (28,29,31-33) reported fractions with 120 kDa, not soluble (80 kDa), E-cadherin. The decrease in E-cadherin in CSC was also supported by the findings of confocal imaging (36) and immunohistochemistry (31,32). However, there have also been controversial studies regarding the expression of E-cadherin in spheroid formation. Transforming GF-beta-induced EMT decreases the expression of E-cadherin in spheroid formation (33,34). E-cadherin enhances CSC-like properties and induces mesenchymal features in colon cancer (37). The overexpression of E-cadherin compromises the EMT-like properties of spheroid formation (32). Spheroid formation in breast cancers depends on the expression of E-cadherin (21). Moreover, Morata-Tarifa *et al* (38) suggested that trypsin-resistant subpopulation showed increased expression of E-cadherin, but trypsin-sensitive subpopulation (EMT-like) represented CSC-like colon cancer cells.

Previous studies have indicated that decreased expression of E-cadherin in cancers may be re-interpreted as the decrease of 120 kDa E-cadherin irrespective of vendors. In the present study, 120 kDa E-cadherin was significantly decreased only in the sphere/FBS of SNU-C5/5-FUR cells. In contrast to expectations, the soluble E-cadherin was significantly increased in the sphere/FBS of both CRC cells as revealed using western blotting and ELISA, which means the essential component of spheroid formation culture was the soluble E-cadherin in FBS-supplemented environment. As the increase in soluble E-cadherin was observed in 28 days after incubation in both CRC cells, it may promote growth and proliferation of spheroids rather than act as an CSCs marker or drug resistance. These findings are confirmed by previous studies that E-cadherin could be a target for spheroid formation or the formation of CSC-like cells in breast cancer (39), and soluble E-cadherin could be an oncogene like EGF when it induces EMT in 3D (24,25,40) as well as in 2D (24) culture environments. Nevertheless, there has been controversy about the mechanism of soluble E-cadherin. The soluble E-cadherin influences invasion via activation of matrix metalloproteinase (MMP), and thus contributes to skin carcinogenesis (24). Exogenous soluble E-cadherin promotes migration and invasion of non-small-cell lung cancer cells, but silencing MMP9 suppresses soluble E-cadherin expression (41). Although ABCG2 could also modulate the expression of E-cadherin in lung cancer (42), ABCG2 did not significantly change in the present study.

Nonetheless, the present study did not reveal the feasible mechanisms of soluble E-cadherin on spheroid formation. As the increase in soluble E-cadherin was observed in long-term maintenance of spheroids, the application of exogenous E-cadherin in spheroid formation culture should be performed to reveal whether soluble E-cadherin is a result or a cause of spheroid formation. If soluble E-cadherin act as an oncogene as it was hypothesized, the possibility of replacement to EGF would be explored based on serial dilution as performed in a recent study (26). Based on these experiments, following signaling pathways of soluble E-cadherin should be further investigated under the more detailed strategy.

In conclusion, spheroid formation culture methods are not appropriate to study CSCs or drug resistance in acquired 5-FU-resistant CRC cells as compared with wild type cells, at least in long-term maintenance condition. Spheroids were easily formed in FBS-supplemented environment via adaptation to anchorage-independent condition, which are related to soluble E-cadherin. These results suggested that soluble E-cadherin could act like an oncogene to grow the spheroids supplemented with FBS, at least in the long-term maintenance condition.

Acknowledgements

Not applicable.

Funding

The present study was supported by the National Research Foundation of Korea (NRF) grant funded by the Korea government (MSIT; grant no. 2021R1F1A1063023).

Availability of data and materials

The datasets used and/or analyzed during the current study are available from the corresponding author on reasonable request.

Authors' contributions

IYC and SPY conceived and designed the present study, performed the experiments for data acquisition and analysis and interpreted the experimental results. IYC and SPY confirm the authenticity of all the raw data. IYC wrote the original manuscript. SPY revised the manuscript. Both authors read and approved the final manuscript and agree to be accountable for all aspects of the research in ensuring that the accuracy or integrity of any part of the work are appropriately investigated and resolved.

Ethics approval and consent to participate

Not applicable.

Patient consent for publication

Not applicable.

Competing interests

The authors declare that they have no competing interests.

References

1. Bray F, Ferlay J, Soerjomataram I, Siegel RL, Torre LA and Jemal A: Global cancer statistics 2018: GLOBOCAN estimates of incidence and mortality worldwide for 36 cancers in 185 countries. CA Cancer J Clin 68: 394-424, 2018.

2. Siegel RL, Miller KD, Fuchs HE and Jemal A: Cancer statistics, 2021. CA Cancer J Clin 71: 7-33, 2021.
3. Kwakman JJ and Punt CJ: Oral drugs in the treatment of metastatic colorectal cancer. Expert Opin Pharmacother 17: 1351-1361, 2016.
4. Stintzing S: Recent advances in understanding colorectal cancer. F1000Res 7: F1000, 2018.
5. Azwar S, Seow HF, Abdullah M, Jabar MF and Mohtarrudin N: Recent updates on mechanisms of resistance to 5-fluorouracil and reversal strategies in colon cancer treatment. Biology (Basel) 10: 854, 2021.
6. Choi CH, Lee TB, Lee YA, Choi S and Kim KJ: Up-regulation of cyclooxygenase-2-derived prostaglandin E(2) in colon cancer cells resistant to 5-fluorouracil. J Korean Surg Soc 81: 115-121, 2011.
7. Kim EJ, Kang GJ, Kang JI, Boo HJ, Hyun JW, Koh YS, Chang WY, Kim YR, Kwon JM, Maeng YH, *et al*: Over-activation of AKT signaling leading to 5-Fluorouracil resistance in SNU-C5/5-FU cells. Oncotarget 9: 19911-19928, 2018.
8. Moon D, Kang HK, Kim J and Yoon SP: Yeast extract induces apoptosis and cell cycle arrest via activating p38 signal pathway in colorectal cancer cells. Ann Clin Lab Sci 50: 31-44, 2020.
9. Kim JW, Kim SH, Mariappan R, Moon D, Kim J and Yoon SP: Anti-cancer effects of the aqueous extract of Orostachys japonica A. Berger on 5-fluorouracil-resistant colorectal cancer via MAPK signalling pathways in vitro and in vivo. J Ethnopharmacol 280: 114412, 2021.
10. Corrò C and Moch H: Biomarker discovery for renal cancer stem cells. J Pathol Clin Res 4: 3-18, 2018.
11. Nguyen LV, Vanner R, Dirks P and Eaves CJ: Cancer stem cells: An evolving concept. Nat Rev Cancer 12: 133-143, 2012.
12. Murphy AJ, Pierce J, de Caestecker C, Ayers GD, Zhao A, Krebs JR, Saito-Diaz VK, Lee E, Perantoni AO, de Caestecker MP and Lovvorn HN III: CITED1 confers stemness to Wilms tumor and enhances tumorigenic responses when enriched in the nucleus. Oncotarget 5: 386-402, 2014.
13. Telang NT: Stem cell models for breast and colon cancer: Experimental approach for drug discovery. Int J Mol Sci 23: 9223, 2022.
14. Liu M, Casimiro MC, Wang C, Shirley LA, Jiao X, Katiyar S, Ju X, Li Z, Yu Z, Zhou J, *et al*: p21CIP1 attenuates Ras- and c-Myc-dependent breast tumor epithelial mesenchymal transition and cancer stem cell-like gene expression in vivo. Proc Natl Acad Sci USA 106: 19035-19039, 2009.
15. Xiao BD, Zhao YJ, Jia XY, Wu J, Wang YG and Huang F: Multifaceted p21 in carcinogenesis, stemness of tumor and tumor therapy. World J Stem Cells 12: 481-487, 2020.
16. Telang N: Drug-resistant stem cells: Novel approach for colon cancer therapy. Int J Mol Sci 23: 2519, 2022.
17. Chang I, Ohn T, Moon D, Maeng YH, Jang BG and Yoon SP: SNU-333 cells as an appropriate cell line for the orthotopic renal cell carcinoma model. Technol Cancer Res Treat 20: 15330338211038487, 2021.
18. Kim JB, Hwang SE and Yoon SP: Dexamethasone reduces side population fraction through downregulation of ABCG2 transporter in MCF-7 breast cancer cells. Mol Med Rep 16: 453-458, 2017.
19. Shibue T and Weinberg RA: EMT, CSCs, and drug resistance: The mechanistic link and clinical implications. Nat Rev Clin Oncol 14: 611-629, 2017.
20. Singla M, Kumar A, Bal A, Sarkar S and Bhattacharyya S: Epithelial to mesenchymal transition induces stem cell like phenotype in renal cell carcinoma cells. Cancer Cell Int 18: 57, 2018.
21. Iglesias JM, Beloqui I, Garcia-Garcia F, Leis O, Vazquez-Martin A, Eguiara A, Cufi S, Pavon A, Menendez JA, Dopazo J and Martin AG: Mammosphere formation in breast carcinoma cell lines depends upon expression of E-cadherin. PLoS One 8: e77281, 2013.
22. Han SJ, Kwon S and Kim KS: Challenges of applying multicellular tumor spheroids in preclinical phase. Cancer Cell Int 21: 152, 2021.
23. Onder TT, Gupta PB, Mani SA, Yang J, Lander ES and Weinberg RA: Loss of E-cadherin promotes metastasis via multiple downstream transcriptional pathways. Cancer Res 68: 3645-3654, 2008.
24. Brouxhon SM, Kyrkanides S, Teng X, Athar M, Ghazizadeh S, Simon M, O'Banion MK and Ma L: Soluble E-cadherin: A critical oncogene modulating receptor tyrosine kinases, MAPK and PI3K/Akt/mTOR signaling. Oncogene 33: 225-235, 2014.
25. Hu QP, Kuang JY, Yang QK, Bian XW and Yu SC: Beyond a tumor suppressor: Soluble E-cadherin promotes the progression of cancer. Int J Cancer 138: 2804-2815, 2016.
26. Zhou G, Lv X, Zhong X, Ying W, Li W, Feng Y, Xia Q, Li J, Jian S and Leng Z: Suspension culture strategies to enrich colon cancer stem cells. Oncol Lett 25: 116, 2023.
27. Gheytanchi E, Naseri M, Karimi-Busheri F, Atyabi F, Mirsharif ES, Bozorgmehr M, Ghods R and Madjd Z: Morphological and molecular characteristics of spheroid formation in HT-29 and Caco-2 colorectal cancer cell lines. Cancer Cell Int 21: 204, 2021.
28. Min SO, Lee SW, Bak SY and Kim KS: Ideal sphere-forming culture conditions to maintain pluripotency in a hepatocellular carcinoma cell lines. Cancer Cell Int 15: 95, 2015.
29. Han XY, Wei B, Fang JF, Zhang S, Zhang FC, Zhang HB, Lan TY, Lu HQ and Wei HB: Epithelial-mesenchymal transition associates with maintenance of stemness in spheroid-derived stem-like colon cancer cells. PLoS One 8: e73341, 2013.
30. Zhang Z, Bu X, Chen H, Wang Q and Sha W: Bmi-1 promotes the invasion and migration of colon cancer stem cells through the downregulation of E-cadherin. Int J Mol Med 38: 1199-1207, 2016.
31. Klopp AH, Lacerda L, Gupta A, Debeb BG, Solley T, Li L, Spaeth E, Xu W, Zhang X, Lewis MT, *et al*: Mesenchymal stem cells promote mammosphere formation and decrease E-cadherin in normal and malignant breast cells. PLoS One 5: e12180, 2010.
32. Tang T, Yang Z, Zhu Q, Wu Y, Sun K, Alahdal M, Zhang Y, Xing Y, Shen Y, Xia T, *et al*: Up-regulation of miR-210 induced by a hypoxic microenvironment promotes breast cancer stem cells metastasis, proliferation, and self-renewal by targeting E-cadherin. FASEB J 6: fj201801013R, 2018.
33. Park NR, Cha JH, Jang JW, Bae SH, Jang B, Kim JH, Hur W, Choi JY and Yoon SK: Synergistic effects of CD44 and TGF-β1 through AKT/GSK-3β/β-catenin signaling during epithelial-mesenchymal transition in liver cancer cells. Biochem Biophys Res Commun 477: 568-574, 2016.
34. Izumiya M, Kabashima A, Higuchi H, Igarashi T, Sakai G, Iizuka H, Nakamura S, Adachi M, Hamamoto Y, Funakoshi S, *et al*: Chemoresistance is associated with cancer stem cell-like properties and epithelial-to-mesenchymal transition in pancreatic cancer cells. Anticancer Res 32: 3847-3853, 2012.
35. Ohnishi Y, Yasui H, Kakudo K and Nozaki M: Lapatinib-resistant cancer cells possessing epithelial cancer stem cell properties develop sensitivity during sphere formation by activation of the ErbB/AKT/cyclin D2 pathway. Oncol Rep 36: 3058-3064, 2016.
36. Acikgoz E, Guven U, Duzagac F, Uslu R, Kara M, Soner BC and Oktem G: Enhanced G2/M arrest, caspase related apoptosis and reduced E-cadherin dependent intercellular adhesion by trabectedin in prostate cancer stem cells. PLoS One 10: e0141090, 2015.
37. Qian Y, Wu X, Yokoyama Y, Okuzaki D, Taguchi M, Hirose H, Wang J, Hata T, Inoue A, Hiraki M, *et al*: E-cadherin-fc chimera protein matrix enhances cancer stem-like properties and induces mesenchymal features in colon cancer cells. Cancer Sci 110: 3520-3532, 2019.
38. Morata-Tarifa C, Jiménez G, García MA, Entrena JM, Griñán-Lisón C, Aguilera M, Picon-Ruiz M and Marchal JA: Low adherent cancer cell subpopulations are enriched in tumorigenic and metastatic epithelial-to-mesenchymal transition-induced cancer stem-like cells. Sci Rep 6: 18772, 2016.
39. Huang S, Cai M, Zheng Y, Zhou L, Wang Q and Chen L: miR-888 in MCF-7 side population sphere cells directly targets E-cadherin. J Genet Genomics 41: 35-42, 2014.
40. Patil PU, D'Ambrosio J, Inge LJ, Mason RW and Rajasekaran AK: Carcinoma cells induce lumen filling and EMT in epithelial cells through soluble E-cadherin-mediated activation of EGFR. J Cell Sci 128: 4366-4379, 2015.
41. Deng X, Chen C, Wu F, Qiu L, Ke Q, Sun R, Duan Q, Luo M and Luo Z: Curcumin inhibits the migration and invasion of non-small-cell lung cancer cells through radiation-induced suppression of epithelial-mesenchymal transition and soluble E-cadherin expression. Technol Cancer Res Treat 19: 1533033820947485, 2020.
42. Liang SC, Yang CY, Tseng JY, Wang HL, Tung CY, Liu HW, Chen CY, Yeh YC, Chou TY, Yang MH, *et al*: ABCG2 localizes to the nucleus and modulates CDH1 expression in lung cancer cells. Neoplasia 17: 265-278, 2015.